NASA Technical Memorandum 81564

KINEMATIC CORRECTION FOR ROLLER SKEWING

Michael Savage
The University of Akron
Akron, Ohio
and
Stuart H. Loewenthal
Lewis Research Center
Cleveland, Ohio

Prepared for the
Sixteenth Biennial Mechanism Conference
sponsored by the American Society
of Mechanical Engineers
Beverly Hills, California, September 29-October 1, 1980

NASA

KINEMATIC CORRECTION FOR ROLLER SKEWING

by

M. Savage, Member ASME
Department of Mechanical Engineering
The University of Akron
Akron, Ohio 44325

and

S.H. Loewenthal, Member ASME
NASA Lewis Research Center
Cleveland, Ohio 44135

E-526

INTRODUCTION

The rollers in a roller bearing tend to skew as they roll around the inner race of the bearing. Roller bearings have shoulders on either inner or outer races to guide the rollers. Needle bearings have a significantly higher tendency to skew, limiting their use to low speed and low shaft misalignment situations [1,2]*. High-speed turbine bearings have a length to diameter ratio of close to one. With this ratio and small clearances between race shoulders and the rollers, a restoring moment is provided at the edges of the roller ends which restrains the roller from skewing. The cage also provides some resistance to the roller skewing through its contact with the roller.

This roller skewing is primarily caused by a dynamic roller imbalance which can be appreciable at the high roller speeds inherent in operation at 2,000,000 DN or higher. (The unit DN, used to identify roller speed, is the bearing bore in millimeters multiplied by its speed in RPM.) Roller skewing induces considerable heat generation and loss of clearance and can lead to bearing seizure at high speeds.

A recent advance in the design of spherical roller bearings [3] uses the friction moments generated in the spherical contacts of the roller with the inner and outer races to resist skewing. Since a condition of pure rolling does not exist in these contacts, the speed of this type of bearing is limited by temperature considerations.

The skewing of rolling elements is a problem which is not restricted to roller bearings. The skewing of flat belts on their pulleys was a problem encountered a century ago which was solved by crowing the pulleys to make the belts crawl up to the center of the pulleys [4]. The solution was based on the elastic nature of the belts in that the restoring moment was due to a gradient in the belt tension across its width. In the centerless grinding

---

* Numbers in brackets denote references in the bibliography.

process the rolling axis of the workpiece and the grinding wheel are deliberately skewed to each other to cause the workpiece to feed through the grinder [5]. Indeed this is a major problem in needle bearings in that a shaft slope at the bearing tends to walk the needles out of the bearing. This is also a problem in traction drives [6] where large thrust forces developed by flanges are required to hold the rolling cylinders in place. The magnitudes of these forces have been studied in the case of a high speed, lightly-loaded cylindrical roller bearing [7]. The effects of shaft misalignment on the roller load distribution has also been studied [8]. Finally, the wheel-rail interaction of railroad car wheel-sets with the rails has plagued designers for a long time [9,10,11]. Flanges are needed on the wheels to provide the significant side forces required to accelerate the cars through the various turns in the road. However, it has been found that the slope of the flanges significantly affects the rolling of the wheels on the rails [11]. Wheels which have a cone apex outside the body of the train are used in order to prevent the wheels from skewing as the train travels along the track. These cones produce a kinematic resistance to skewing which the internal apex cones with flanges outboard of the rail would not.

In this paper, a kinematic stability criterion is investigated and defined. This analysis extends the stability model developed in [12,13]. It is applied to determine the basic roller bearing geometries which provide kinematic stabilization through one race while allowing free axial motion at the other. These bearings all have one straight race and one contoured race for stability. Two levels of roller complexity are considered. The first is a simple roller with a single transverse convex curvature. There are four bearing geometries which use this roller. The second is a compound roller with a central band of constant radius. This radius is the largest radius of the roller. This central band is flanked by two symmetric bands with transverse curvature. The roller transverse curvature may be convex, straight or concave. Eight additional bearing geometries employ these compound rollers.

STABILITY THEORY

The basic model for rolling contact in a cylindrical roller bearing assumes that no skewing can take place since the axes of the rollers and races remain parallel. It further assumes that the races and the roller are perfect cylinders with constant radii along the length of their axes. Thus, a single plane rolling model is used. This model is valid as long as the axes remain parallel.

In reality, the rolling surfaces are not uniform. The axes are not perfectly parallel. And roller contact occurs in more than one plane. The actual contact is not pure rolling but a complex combination of rolling and sliding across the face of the roller.

To establish the primary cause of skewing, this contact is modeled in two planes instead of the single plane of the basic roller model. This two plane model allows for rolling and sliding at the individual planes and a resultant generation of a skewing torque due to variations in rolling geometry from one plane to the other.

In this model consider roller "a" to represent the rolling element, roller "b" to represent the inner race and roller "c" to represent the outer race of the bearing. The races rotate about fixed axes with no axial motion. Plane 1 is at the small end of the rolling element roller a. For equal and opposite slip in the two planes, the radius at which true rolling would occur is the average of the two rolling radii of roller a.

Figure 1 illustrates the rolling contact of the rolling element with the inner race. As shown in the velocity drawing, roller b slips ahead of roller a at the contact point in plane 1 while the relative velocity is reversed in plane 2 and roller a slips ahead of roller b. These two skidding velocities

produce a counterclockwise tractive couple on roller a which tends to push its plane 1 into the paper and pull its plane 2 out of the paper. This skewing turns the relative velocity of the center of roller a with respect to roller b slightly towards plane 1. The axial component of this velocity is thus an axial motion of roller a on roller b. If this motion decreases the ratio r_{1b}/r_{1a} and increases the ratio r_{2b}/r_{2a}, the skidding velocities will be reduced and even reversed when r_{1a} and r_{1b} pass the mean value. Assuming this antisymmetric behavior, the total stability or tendency to self correct without external forces can be measured by the inequality

$$\frac{\partial}{\partial z}\left(\frac{r_{1b}}{r_{1a}}\right) < 0 \qquad (1)$$

where z measures the axial motion of roller a and is positive for motion toward plane 1 [12].

In a similar fashion, figure 2 illustrates the rolling contact of the rolling element with the outer race. As shown in the velocity drawing, roller c slips ahead of roller a in plane 1 and slips behind roller a in plane 2. The sliding tendency is not as great in this case since both centers of rotation are on the same side of the pitch point. However, it is still there and in the same direction as in the previous case. For the same direction of rotation of the race c in this case as that of the race b in the previous case, the angular velocity of the roller a reverses but the relative velocity of its center with respect to the race is also out of the paper. Thus, a similar counterclockwise tractive torque produces the same skewing and axial motion toward plane 1 - the small end of the roller. If this motion decreases the ratio r_{1c}/r_{1a} and increases the ratio r_{2c}/r_{2a} the skidding velocities will be reduced as before. An equivalent stability criterion can thus be stated as

$$\frac{\partial}{\partial z}\left(\frac{r_{1c}}{r_{1a}}\right) < 0 \qquad (2)$$

INNER RACE STABILITY

The stability or self correcting action of the roller with the inner race is determined by applying the criterion of equation 1 to the possible transverse profiles for the roller and inner race. These profiles must be axially symmetric about the center plane of the roller and inner race. They must also afford only one contact point between the roller and race on each side of this center plane. The geometric combinations that satisfy this are:

1) convex - convex

2) convex - straight, and

3) convex - concave.

In these three cases, the rolling element may be either the first or second item. A fourth combination must be included which does not possess two definite contact points in order to include present bearings. That is:

4) straight - straight.

Initially, the contact geometry will be looked at irrespective of which roller is the inner race and which is the rolling element.

In the case of two convex surfaces, the axial motion will be such as to maintain the distance between the centers of transverse curvature, considering the geometric effect of skewing to be negligible. In the analysis to follow, ρ is the transverse radius of curvature, r is the rolling radius and R is the radial distance from the roller's spin axis to the center of transverse curvature. If $\rho \cos \alpha$ is less than r, R is positive. The angle α is the inclination of the contact normal from the radial direction. It is also the angle that describes the contact slope relative to the axial direction. In

each of the cases examined, roller e will be the roller that has the apex of its conical surfaces outboard of its main body for positive α in plane 1.

Figure 3 shows two cylinders in contact, both of which have transverse convex surfaces. The a cylinder is shown in two adjacent positions to clarify the effect of the axial motion dz on the contact geometry. In this case the effect is to increase α by the angle $d\alpha$. If C is defined as the center distance of transverse curvature, then

$$C = \rho_d + \rho_e \tag{3}$$

and the slope angle α is related to z by

$$\sin \alpha = \frac{z}{C} \tag{4}$$

and

$$\cos \alpha = \frac{\sqrt{C^2 - z^2}}{C} \tag{5}$$

The contact radii are given by

$$r_{1d} = R_d + \rho_d \cos \alpha \tag{6}$$

and

$$r_{1e} = R_e + \rho_e \cos \alpha \tag{7}$$

Thus

$$\frac{r_{1e}}{r_{1d}} = \frac{R_e + \rho_e \cos \alpha}{R_d + \rho_d \cos \alpha} \tag{8}$$

For stability

$$\frac{\partial}{\partial z} \left(\frac{r_{1e}}{r_{1d}} \right) < 0 \tag{9}$$

After some differentiation and the appropriate algebra,

$$\frac{\partial}{\partial z} \left(\frac{r_{1e}}{r_{1d}} \right) = (r_{1e}\rho_d - r_{1d}\rho_e) \frac{\tan \alpha}{C r_{1d}^2} \tag{10}$$

The sign of this expression is controlled by $(r_{1e}\rho_d - r_{1d}\rho_e) \tan \alpha$, which indicates kinematic stability according to equation (1) when it is negative. For a positive α (as drawn in fig. 3) stability occurs when

$$r_{1e}\rho_d < r_{1d}\rho_e \tag{11}$$

or

$$\frac{r_{1e}}{r_{1d}} < \frac{\rho_e}{\rho_d} \tag{12}$$

For positive α the e roller has the apex of its conical contact surface outboard of the roller ends as shown in figure 3. Since the transverse curvature of roller d is shown to be significantly smaller than that of roller e, kinematic stability can be expected even though the rolling radii of both bodies are nearly the same. However, if the radii of transverse curvature happen to be nearly equal, the rolling radius of the e roller must be smaller than that of the mating roller d for definite kinematic stability. For the double convex contact, it can be stated that the kinematic stability is defined by the sign of equation (10).

Figure 4 shows two rollers in contact: one has convex transverse curvature, and the other has a straight transverse profile. In this case C is infinite, so a slight modification is required in the previous analysis. Equation (7) still holds but the rolling radius of the straight coned roller becomes

$$r_{1e} = r_{oe} - z \tan \alpha \tag{13}$$

where r_{oe} is the nominal rolling radius of that roller at the plane in which z has a zero value. The ratio of rolling radii in plane 1 becomes

$$\frac{r_{1e}}{r_{1d}} = \frac{r_{oe} - z \tan \alpha}{R_d + \rho_d \cos \alpha} \tag{14}$$

Note that in this case, the angle α, the inclination of the contact, is constant with changes in z since the shape of the straight cone does not change along its surface. For stability in accordance with equation (1), differentiation of equation (13) yields

$$\frac{\partial}{\partial z}\left(\frac{r_{1e}}{r_{1d}}\right) = -\frac{\tan \alpha}{r_{1d}} \tag{15}$$

where stability is insured for this set of contacts as long as the angle α is positive as drawn. Thus, the cone shaped roller must be the one with the apex outboard of its main body. In this case the radii of transverse curvature dictate stability, since one is infinite and the other is finite. This can be appreciated by setting ρ_e equal to infinity in equation (12).

The third case of roller combinations is shown in figure 5. Here roller d has convex transverse curvature along its contact surfaces, and roller e has concave transverse curvature. This condition makes ρ_e negative and greater than ρ_d in absolute value, so C from equation (3) is also negative. This also makes z negative for the geometry as shown but equation (10) is still applicable with the use of a negative radius of transverse curvature ρ_e for the concave surface. The sign is again determined by $(r_{1e}\rho_d - r_{1d}\rho_e)\ (\tan \alpha)/Cr_{1d}^2$ where C is no longer positive definite.

Since C is negative and α is positive for the geometry as drawn, stability is defined by

$$r_{1e}\rho_d - r_{1d}\rho_e > 0 \tag{16}$$

or

$$\frac{r_{1e}}{r_{1d}} > \frac{\rho_e}{\rho_d} \tag{17}$$

Since ρ_d is positive and ρ_e is negative by definition of the transverse curvature, the drawn geometry is stable for positive α. A reversed cone slope, that is, negative α, would make this contact unstable. The railroad wheel-rail contact is in agreement with this criterion.

The last contact pair to be considered is that of two straight sided cylinders. Figure 6 illustrates this condition. As in the second case, assign the nominal rolling radii the symbols r_{od} and r_{oe}. The angle α is the cone half angle or the inclination of the cone surface to the axes and z denotes the axial travel of cylinder d relative to e to the right. Unlike the previous cases, no kinematically defined point of rolling contact exists to identify plane 1. Assume that this plane is located at the midpoint of the contact of the spool model. Thus r_{od} and r_{oe} become the radii at the contact center and

$$r_{1d}=r_{od}-\frac{z}{2}\tan\alpha \tag{18}$$

$$r_{1e}=r_{oe}-\frac{z}{2}\tan\alpha \tag{19}$$

Note that both rolling radii decrease with relative axial travel z. Thus, the radius ratio becomes

$$\frac{r_{1e}}{r_{1d}}=\frac{r_{oe}-\frac{z}{2}\tan\alpha}{r_{od}-\frac{z}{2}\tan\alpha} \tag{20}$$

and

$$\frac{\partial}{\partial z}\left(\frac{r_{1e}}{r_{1d}}\right)=(r_{1e}-r_{1d})\frac{\tan\alpha}{2r_{1d}^2} \tag{21}$$

which is quite similar to equation (10). As before, the sign is controlled by $(r_{1e}-r_{1d})\tan\alpha$ since r_{1d}^2 is always positive.

As drawn, the angle α is positive and stability is defined by

$$r_{1d}>r_{1e} \tag{22}$$

Thus, a stable contact of straight sided cylinders would have the larger radius cylinder taper inward. Equal radii cylinders would be neutrally stable and, thus, have no restoring properties. Neutral stability exists for straight cylinders with no taper regardless of the value of the rolling radii. This is a direct consequence of $\tan\alpha = 0$, so that

$$\frac{\partial}{\partial z}\left(\frac{r_{1e}}{r_{1d}}\right) = \frac{\partial}{\partial z}\left(\frac{r_{2e}}{r_{2d}}\right) = 0 \tag{23}$$

for the taperless cylinders.

Table 1 summarizes the stability conditions for rollers in free rolling contact where both rolling surfaces are on the outside of their respective cylinders. This contact is of external - external rollers.

Table 2 shows these results in a form more easily applied to the bearing design problem at hand. In this expanded table, roller a is the rolling element and roller b is the inner race of the bearing. The cone angle of transverse curvature, α, is considered positive if the cone apex of roller a is outside of the roller as is the case for roller e.

OUTER RACE STABILITY

In a similar fashion, the stability of the roller with the outer race is determined by applying the criteria of equation 2 to the transverse profiles.

These profiles must be axially symmetric about the center plane of the roller and outer race. They must also afford only one contact point between the roller and race on each side of this center plane. Each combination must be considered separately. Listing the roller transverse curvature first and the outer race transverse curvature second, these contact combinations are:

1) convex - convex
2) convex - straight
3) convex - concave
4) straight - convex
5) straight - straight, and
6) concave - convex.

These cases are treated with the following nomenclature. The slope of the transverse curvature is identified by the angle α which is positive for external cone apexes on roller a. The radius of transverse curvature, ρ, is positive for convex and negative for concave surfaces. The rolling radius, r, and radius to the center of transverse curvature, R, are both positive when directed from the center of roller rotation toward the contact point and negative when opposite. A positive dz identifies motion of roller a towards plane 1 as before. The center distance of transverse curvature is

$$C = \rho_a + \rho_c \tag{24}$$

Figure 7 shows the geometry of the first case, convex - convex. The slope angle, α, is related to the axial position of roller a by

$$\sin \alpha = \frac{-z}{C} \tag{25}$$

In plane 1 the two rolling radii are given by

$$r_{1a} = R_a + \rho_a \cos \alpha \tag{26}$$

and

$$r_{1c} = R_c - \rho_c \cos \alpha \tag{27}$$

Thus

$$\frac{r_{1c}}{r_{1a}} = \frac{R_c - \rho_c \cos \alpha}{R_a + \rho_a \cos \alpha} \tag{28}$$

and assuming that the radial shift of the roller axis is negligible compared to the axial roller shift

$$\frac{\partial}{\partial_z} \left(\frac{r_{1c}}{r_{1a}}\right) = - \left(r_{1a}\rho_c + r_{1c}\rho_a\right) \frac{\tan \alpha}{C\, r_{1a}^2} \tag{29}$$

Since every length in this geometry is positive, this case is determined solely by the sign of the slope angle,

$$\frac{-(r_{1a}\rho_c + r_{1c}\rho_a) \tan \alpha}{C\, r_{1a}^2} < 0 \tag{30}$$

for positive α values or slopes as drawn in Figure 7.

Figure 8 shows the geometry for the second case, convex - straight. In this case the slope angle is constant and the rolling radii are given by

$$r_{1a} = R_a + \rho_a \cos \alpha \tag{31}$$

$$r_{1c} = r_{oc} - z \tan \alpha \tag{32}$$

where z has a value of zero in the initial position. A second difference of the straight cone cases from the others is that z is referenced at the contact point directly and not at a center of transverse curvature of the surface. The quantity r_{oc} is the rolling radius of the outer race in plane 1 in the initial position. Thus

$$\frac{r_{1c}}{r_{1a}} = \frac{r_{oc} - z \tan \alpha}{R_a + \rho_a \cos \alpha} \tag{33}$$

and

$$\frac{\partial}{\partial z} \left(\frac{r_{1c}}{r_{1a}}\right) = - \frac{\tan \alpha}{r_{1a}} \tag{34}$$

Once again this is controlled by the sign of the angle α, so

stability is obtained with a positive angle α as shown in Figure 8

$$-\frac{\tan \alpha}{r_{1a}} < 0 \tag{35}$$

Figure 9 shows the geometry for the third case, convex - concave. The slope angle, α, is defined by equation 25 and the two rolling radii are given by equations 26 and 27. Thus, the analysis of this case is the same as that for the convex - convex case. However, since ρ_c is negative, the stability conclusions to be drawn from equation 9 change slightly. Since $|\rho_c|$ must be greater than ρ_a, C is negative and

$$(r_{1a}\rho_c + r_{1c}\rho_a) \tan \alpha < 0 \tag{36}$$

Thus two possible stable conditions result.

$$\frac{r_{1c}}{r_{1a}} < \left|\frac{\rho_c}{\rho_a}\right| \quad \text{and } \alpha > 0 \tag{37}$$

or

$$\frac{r_{1c}}{r_{1a}} > \left|\frac{\rho_c}{\rho_a}\right| \text{ and } \alpha < 0 \tag{38}$$

In either case the two factors offset each other so the stability is not as great as that of the first two cases.

Figure 10 shows the geometry for the fourth case, straight - convex. As in the second case, the slope angle α is a constant. The rolling radii are given by:

$$r_{1a} = r_{oa} + z \tan \alpha \tag{39}$$

and

$$r_{1c} = R_c - \rho_c \cos \alpha \tag{40}$$

Thus

$$\frac{r_{1c}}{r_{1a}} = \frac{R_c - \rho_c \cos \alpha}{r_{oa} + z \tan \alpha} \tag{41}$$

and

$$\frac{\partial}{\partial z}\left(\frac{r_{1c}}{r_{1a}}\right) = -\frac{r_{ic}\tan\alpha}{r_{1a}^2} \tag{42}$$

Since r_{1c} is always positive then stability is once again determined primarily by the sign of the slope angle α.

$$-\frac{r_c\tan\alpha}{r_{1a}^2} < 0 \tag{43}$$

for positive values of α and is not true for negative values.

Figure 11 shows the geometry for the fifth case, straight - straight. This case differs from the other five in that kinematically defined contact points do not exist. If it is assumed that the contact point remains in the center of the contact region and that the contact pressure remains nearly uniform then the rolling radii can be expressed as

$$r_{1a} = r_{oa} + \frac{z}{2}\tan\alpha \tag{44}$$

and

$$r_{1c} = r_{oc} - \frac{z}{2}\tan\alpha \tag{45}$$

Where the slope angle α is a constant and the two radii r_{oa} and r_{oc} are the initial rolling radii in plane 1.

The ratio is thus

$$\frac{r_{1c}}{r_{1a}} = \frac{r_{oc} - \frac{z}{2}\tan\alpha}{r_{oa} + \frac{z}{2}\tan\alpha} \tag{46}$$

and its derivative with respect to z is

$$\frac{\partial}{\partial z}\left(\frac{r_{1c}}{r_{1a}}\right) = \frac{-(r_{1c} + r_{1a})\tan\alpha}{2(r_{1a})^2} \tag{47}$$

Stability is thus defined by

$$\frac{-(r_{1c} + r_{1a})\tan\alpha}{2r_{1a}^2} < 0 \tag{48}$$

which is satisfied for positive α and not satisfied for negative α values.

If it is assumed that the contact points shift to the right hand edge of roller c's surfaces then roller a will continue to roll to the right without correction since a fixed imbalance will exist between the rolling radii r_{1c} and r_{2c} of the outer ring.

If it is assumed that the contact points shift to the left hand edges of roller a, then the imbalance will be between the rolling radii r_{1a} and r_{2a} of the roller. This imbalance will shift the roller to the left until contact on these edges is no longer possible at which time the roller might be shifted back to the right by the aforementioned outer ring edge rolling contact.

In any case, if edge rolling contact occurs on the straight cases, instabilities at least to the point of limit cycle oscillations will occur.

Figure 12 shows the geometry for the sixth and final case, concave-convex. As in the third case, the first analysis applies with the awareness of a sign change. The radius of transverse curvature of the roller, ρ_a, is negative and greater in magnitude than the radius of transverse curvature of the outer race, ρ_c. This makes C negative and results in the condition of equation 36 for stability. Since r_{1c} is greater than r_{1a}, the second term is much larger than the first. Since this term is negative, stability is determined by the sign of the slope angle α. A positive value indicates stability while a negative value indicates instability.

Table 3 is a summary of the stability conditions for the six cases of roller-outer race contact, assuming mid-point contact for the straight sided rollers. It is interesting to note that the stability criterion for all ten cases of inner- and outer- race contact listed in tables 3 and 4 can be expressed in a simple inequality if the radius of the outer race if considered to be negative. Considering r_{1x} equal to r_{1b} and ρ_x equal to ρ_b for inner-race contact and r_{1x} equal to $-r_{1c}$ and ρ_x equal to ρ_c for outer race contact, this expression becomes:

$$\frac{-(r_{1a}\rho_x - r_{1x}\rho_a)}{(\rho_x + \rho_a)r_{1a}^2} \tan \alpha < 0 \qquad (49)$$

The relative stability of the different contacts can be compared directly using this relation.

STABLE ROLLER BEARING GEOMETRIES

A roller bearing must allow free axial motion of the supported shaft with respect to the housing. To do this, one race rolling surface must be straight or parallel to the shaft centerline. The roller must have a single rolling band as its largest radius to contact that race rolling surface. To minimize the restriction to shaft slope or misalignment, this rolling band should be located in the center of the roller. Two levels of roller complexity are considered in this work: (1) a single convex transverse curvature with zero slope at the center as shown in Figure 13, and (2) a compound transverse slope composed of a central cylinder with the largest rolling radius flanked by two symmetric transverse curvatures which have tangent cones with apexes outside the roller center as shown in Figure 14. In both roller configurations, the roller cone angle, α, must be positive.

Table 4 lists the twelve possible stable bearing configurations which these restrictions allow. The type of transverse curvature on the coned surfaces is listed in the table. The straight cylindrical race of constant radius is noted by the word neutral under inner or outer race curvature for each bearing in the table. For the four bearings for which the stability is listed as conditional, the radii of transverse curvatures must satisfy an inequality for the geometry to be stable. Geometries which require straight cones to contact straight cones are considered unstable due to the cornering effects of their contact.

These twelve bearings with simple and compound rollers which provide kinematic stabilization are illustrated in Figures 13 and 14. Figure 13 shows the basic restoring geometry of the four simple roller bearings. Each figure represents the geometry of a simple roller bearing. A corresponding com-

pound roller bearing with similar convex curvature on its two outer bands and a straight central band exists for each simple roller bearing shown in figure 13. Figure 14 shows the basic restoring geometry of the last four compound roller bearings which have no simple roller counterpart.

The first four bearings in Table 4 represent the only possible stable combination of a convex roller with either an inner or an outer contoured race surface. The final eight bearings extend this class of stable bearings by introducing the first level of compound roller curvature. They represent the only stable bearings with symmetric single curvature restoring surfaces. It is important to note that for each of these geometries, the roller is contained by both the inner and outer races with three contact points in the transverse plane. Thus, its position will be well defined and solid contact at each point is assured. The next level of roller complexity is variable radii of transverse curvature. This geometry is considered beyond the scope of the present work and will not be considered here. However, it should be investigated as the bearing designs are refined.

VERIFICATION

To verify this kinematic theory of roller skewing and skew correction low speed tests were conducted with high-cone angle rollers. Six rollers were made with symmetry about their central planes. These rollers were made in three sets of two each - one with a positive cone angle and one with a negative cone angle. The first set had straight sided cones, the second had cones with convex transverse curvature while the third had cones with concave transverse curvature. Two straight dowels of small transverse curvature were then placed side by side as a downward ramp of infinite radius. In

tables 2 and 3 it can be seen that the three rollers with positive cone angles should be stable while those with negative cone angles should be unstable. This was the behavior noted. The rollers with the positive taper rolled down to the bottom of the ramp with a decreasing sideways oscillation. The rollers with the negative taper rolled sideways off the ramp before they could reach the bottom.

Two major differences exist between this situation and that of a roller in a bearing. First, the roller contacts both the inner and outer races, so the potential exists for kinematic skewing or skew correction in two contacts. In the spherical roller bearing this occurs with the spin in one race fighting that of the other. One property of the cylindrical roller bearing which must be maintained is that of free axial motion of the inner race with respect to the outer race. This can be maintained by leaving a neutral contact with a straight, constant radius cylindrical race at either the inside race or the outside race. Thus, the proposed bearing designs offer kinematic skew correction at the contact with one race and neutral contact with the other.

Secondly, the roller is trapped in a fixed clearance. When the roller moves axially, the radial stiffness of the bearing produces high-contact pressures due to wedging. These pressures tend to restrain further motion. As noted in the stability theory development, the skewing of the roller is produced by a spin torque due to the relative differential slip within the contacts. This torque, resulting from tractive forces generated in the contact, has been modeled in [13]. A similar relationship between spin torque and skew has also been developed in [3] for spherical roller bearings. In this reference, bearing power loss and roller skew measurements for

spherical roller bearings with anti-skew corrective geometry have confirmed the beneficial effects of controlling roller skewing. These analyses and measurements confirm that bearings with proper kinematic design will have reduced wedging of their rollers due to skewing. This reduced wedging will cause longer bearing life, lower power loss and reduced heat generation especially in high-speed applications.

BEARING DESIGN

In applying these criteria to the design of a roller bearing, one must consider the design compromise between radial capacity and skew correcting torque. The radial capacity can be estimated from Hertzian contact stress calculations. The restoring torque can be estimated from the slip velocities at the contact points and the traction coefficients which relate shear force to slip velocity.

For a single curvature roller, the cone angle at the contact point and the radius of curvature of the roller are directly tied to the roller's width. The need for reasonably large radii of transverse curvature to provide the required radial capacity of the bearing causes the cone angle to be very small. This limits the magnitude of the restoring torque and allowable roller imbalance.

This leads one to consider the second level of complexity in the rollers. That is a central band of uniform radius for radial capacity flanked by two symmetric bands of transverse curvature to provide the kinematic skew correction. This enables both the radius of transverse curvature and the cone angle to be larger. Thus,high radial capacity can be maintained while a high degree of kinematic skew correction is obtained. The magnitude of the cone angle should still be kept relatively small, however, to maintain low bearing power loss and heat generation due to spin in the contact region. This spin

is a system of differential slip velocities which exist circumferentially in the contact zone between the tapered rollers. The analysis of [14] indicates that a small amount of spin, hence roller taper, can be tolerated without an appreciable effect on power loss. The cone angle should be selected to produce an optimal combination of maximum bearing life and stability with minimum power loss. Figure 15 illustrates one design for an experimental high speed roller bearing which maintains the low speed radial capacity while providing significant skew stability.

SUMMARY OF RESULTS

A theory of kinematic stabilization of rolling cylinders was developed and applied to the design of cylindrical roller bearings. This theory predicts and helps prevent axial motion of free rolling cylinders.

The theory includes external-external roller contact and internal-external roller contact. It incorporates three basic parameters which affect the kinematic stability of free rolling roller pairs. These three parameters are:

1) The half cone slope angle α,

2) The rolling radius ratio r_b/r_a or r_c/r_a and

3) The transverse curvature ratio ρ_b/ρ_a or ρ_c/ρ_a.

Low speed, free rolling tests were performed to verify this analysis. The analysis was used to develop a complete table of restoring geometries for roller contact with either inner or outer bearing races. The following results were obtained:

1. The inter-relationship of the above three parameters in producing axial stability or instability can be represented by a single relation as follows:

$$\frac{-(r_{1a}\rho_x - r_{1x}\rho_a)}{(\rho_x + \rho_a)r_{1a}^2} \tan \alpha < 0$$

2. A set of four stable bearing geometries with single transverse roller curvature can be designed. In addition, a set of eight stable bearing geometries can be designed which utilize three bands of curvature that are symmetric about the roller center plane.

3. Low speed tests of these geometries have verified that the simplified two plane rolling model is adequate to predict the presence of axial stability or instability in cylindrical rolling.

ACKNOWLEDGEMENT

This work was supported in part under NASA Lewis Research Center grant NSG 3077 managed by David E. Brewe.

NOMENCLATURE (Savage and Loewenthal)

Variables

C transverse curvature center distance in milimeters

O center of transverse rotation

R radius to center of transverse curvature in milimeters

r rolling radius in milimeters

U slip velocity in milimeters per second

V total velocity in milimeters per second

z axial roller direction

α half cone angle in degrees

ρ radius of transverse curvature in milimeters

ω angular velocity in radians per second

Subscripts

a roller

b inner race

c outer race

d external rolling cylinder

e external rolling cylinder

o nominal rolling value

1,2 right and left sides of roller

BIBLIOGRAPHY

1. Palmgren, A., Ball and Roller Bearing Engineering, 3rd ed., SKF Industries, Burbank, 1959.

2. Harris, T. A., Rolling Bearing Analysis, John Wiley, New York, 1966, pp. 95-109.

3. Kellstrom, E. M., "Rolling Contact Guidance of Rollers in Spherical Roller Bearings," ASME Paper 79-LUB-23, Oct. 1979.

4. Swift, H. W., "Cambers for Belt Pulleys," Proc. Instn. Mech. Engrs., Vol. 122, 1932, pp. 627-671.

5. Woodbury, R. S., History of the Grinding Machine. M.I.T. Press, Cambridge, 1959.

6. Virabov, R. V., "Influence of Shaft Misalignment on Friction-Drive Tractive Properties," Russian Engineering Journal, Vol. 53, No. 7, 1973, pp. 20-24.

7. Korrenn, H., "The Axial Load-Carrying Capacity of Radial Cylindrical Roller Bearings," Journal of Lubrication Technology, Vol. 92, No. 1, Jan. 1970, pp. 129-137.

8. Liu, J. Y., "The Effect of Misalignment on the Life of High Speed Cylindrical Roller Bearings," Journal of Lubrication Technology, Vol. 93, No. 1, Jan. 1971, pp. 60-67.

9. Milenkovic, V., "The Generalized Problem of Lateral Guidance Stability in Wheeled Vehicle," Mechanical Engineering, Vol. 92, No. 12, Dec. 1970, Abstract No. 70-TRANS-17, p. 62.

10. Wickens, A. H., "The Dynamics of Railway Vehicles on Straight Track: Fundamental Considerations of Lateral Stability." Proceedings of Institution of Mechanical Engineers, Vol. 180, pt. 3F, 1965-1966, pp. 29-44.

11. Cooperrider, N. K., "The Hunting Behavior of Conventional Railway Trucks," Journal of Engineering for Industry, Vol. 94, No. 2, May 1972, pp. 752-762.

12. Savage, M. and Loewenthal, S. H., "Kinematic Stability of Roller Pairs in Free-Rolling Contact," NASA TN D-8146, 1976.

13. Savage, M. and Pinkston, B. H. W., "Roller Bearing Geometry Design," Case Western Reserve University, Cleveland, Ohio, Oct. 1976. (NASA CR-135082.)

14. Tevaarwerk, J. L., "Traction Drive Performance Prediction for the Johnson and Tevaarwerk Traction Model," NASA TP 1530, 1979.

TABLE 1. - AXIAL STABILITY CRITERIA OF EXTERNAL-EXTERNAL CONTACT ROLLERS

Roller Curvature Geometry Roller d - Roller e	Roller e Outboard Apex (+ α)	Roller d Outboard Apex (- α)
convex - convex	$\frac{r_{1e}}{r_{1d}} < \frac{\rho_e}{\rho_d}$	$\frac{r_{1e}}{r_{1d}} > \frac{\rho_e}{\rho_d}$
convex - straight	yes	no
convex - concave	yes	no
straight - straight	$\frac{r_{1e}}{r_{1d}} < 1$	$\frac{r_{1e}}{r_{1d}} > 1$

TABLE 2. - STABILITY CRITERIA APPLIED TO INNER RACE CONTACT

Roller Curvature (Roller a)	Inner Race Curvature (Inner Race - b)	Roller a With Outboard Apex ($+\alpha$)	Roller a With Inboard Apex ($-\alpha$)
convex	convex	$\frac{r_{1a}}{r_{1b}} < \frac{\rho_a}{\rho_b}$	$\frac{r_{1a}}{r_{1b}} > \frac{\rho_a}{\rho_b}$
convex	straight	no	yes
convex	concave	no	yes
straight	convex	yes	no
straight	straight	$\frac{r_{1a}}{r_{1b}} < 1$	$\frac{r_{1a}}{r_{1b}} > 1$
concave	convex	yes	no

TABLE 3. - STABILITY CRITERIA APPLIED TO OUTER RACE CONTACT

Roller Curvature (Roller a)	Outer Race Curvature (Outer Race - c)	Roller a With Outboard Apex ($+\alpha$)	Roller a With Inboard Apex ($-\alpha$)
convex	convex	yes	no
convex	straight	yes	no
convex	concave	$\frac{r_{1c}}{r_{1a}} < \left\lvert\frac{\rho_c}{\rho_a}\right\rvert$	$\frac{r_{1c}}{r_{1a}} > \left\lvert\frac{\rho_c}{\rho_a}\right\rvert$
straight	convex	yes	no
straight	straight	yes	no
concave	convex	yes	no

TABLE 4. - STABLE BEARINGS

Roller Type	Roller Curvature	Inner Race Curvature	Outer Race Curvature	Stability	Figure No.
simple	convex	convex	neutral	conditional	13a
		neutral	convex	stable	13b
		neutral	straight	stable	13c
		neutral	concave	conditional	13d
compound	convex	convex	neutral	conditional	13a*
		neutral	convex	stable	13b*
		neutral	straight	stable	13c*
		neutral	concave	conditional	13d*
	straight	convex	neutral	stable	14a
		neutral	convex	stable	14b
	concave	convex	neutral	stable	14c
		neutral	convex	stable	14d

*As shown except with a straight central band added to the roller.

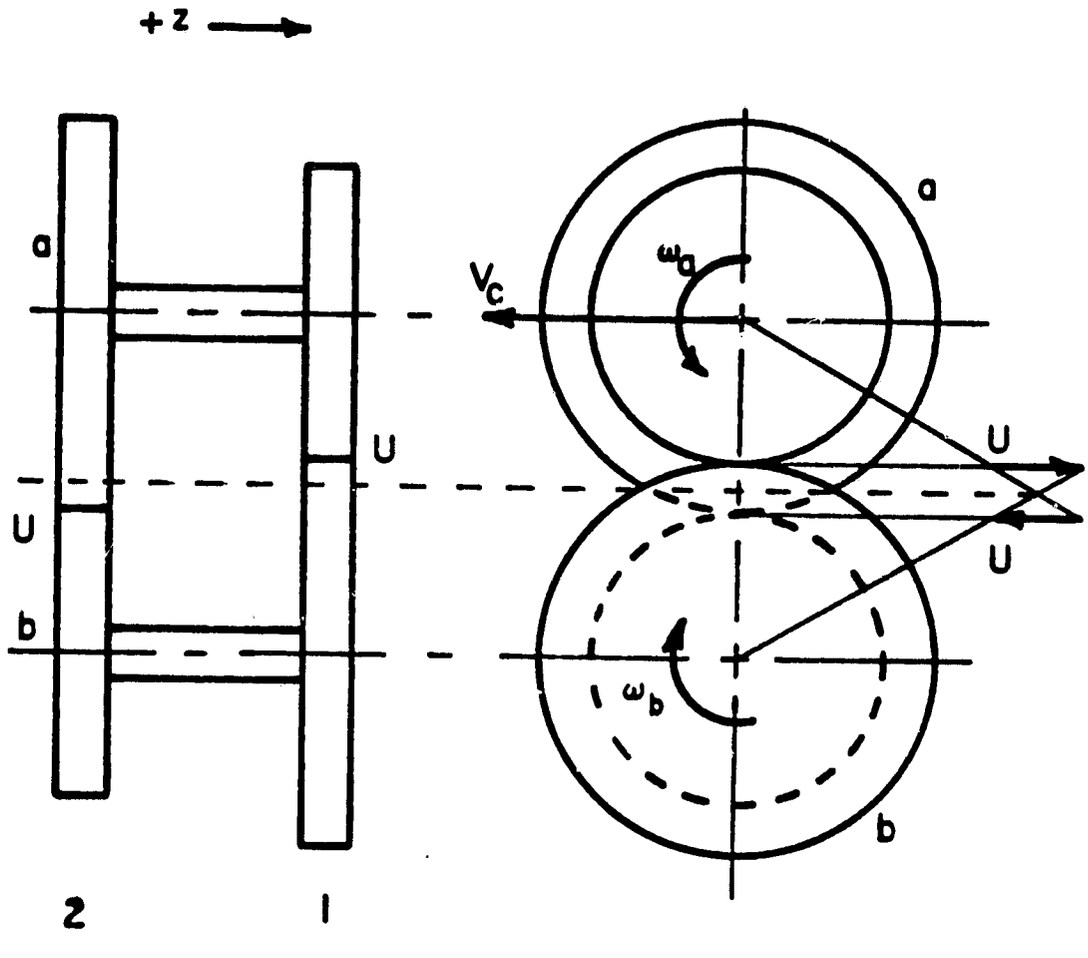

Figure 1 Roller-Inner Race Skewing Model

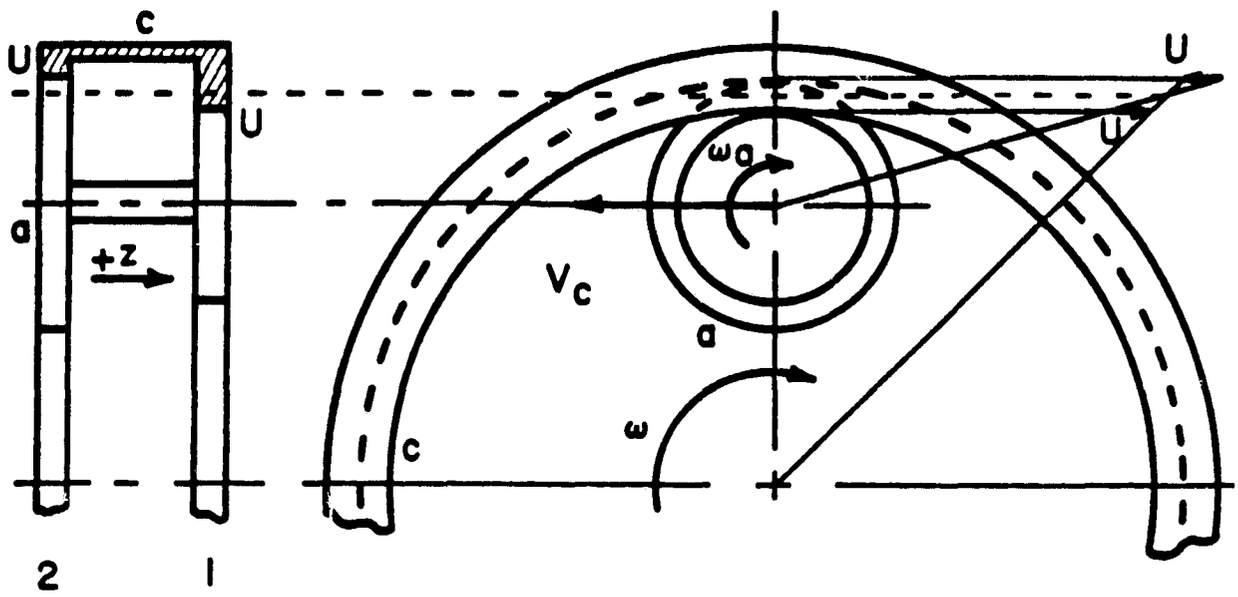

Figure 2 Roller-Outer Race Skewing Model

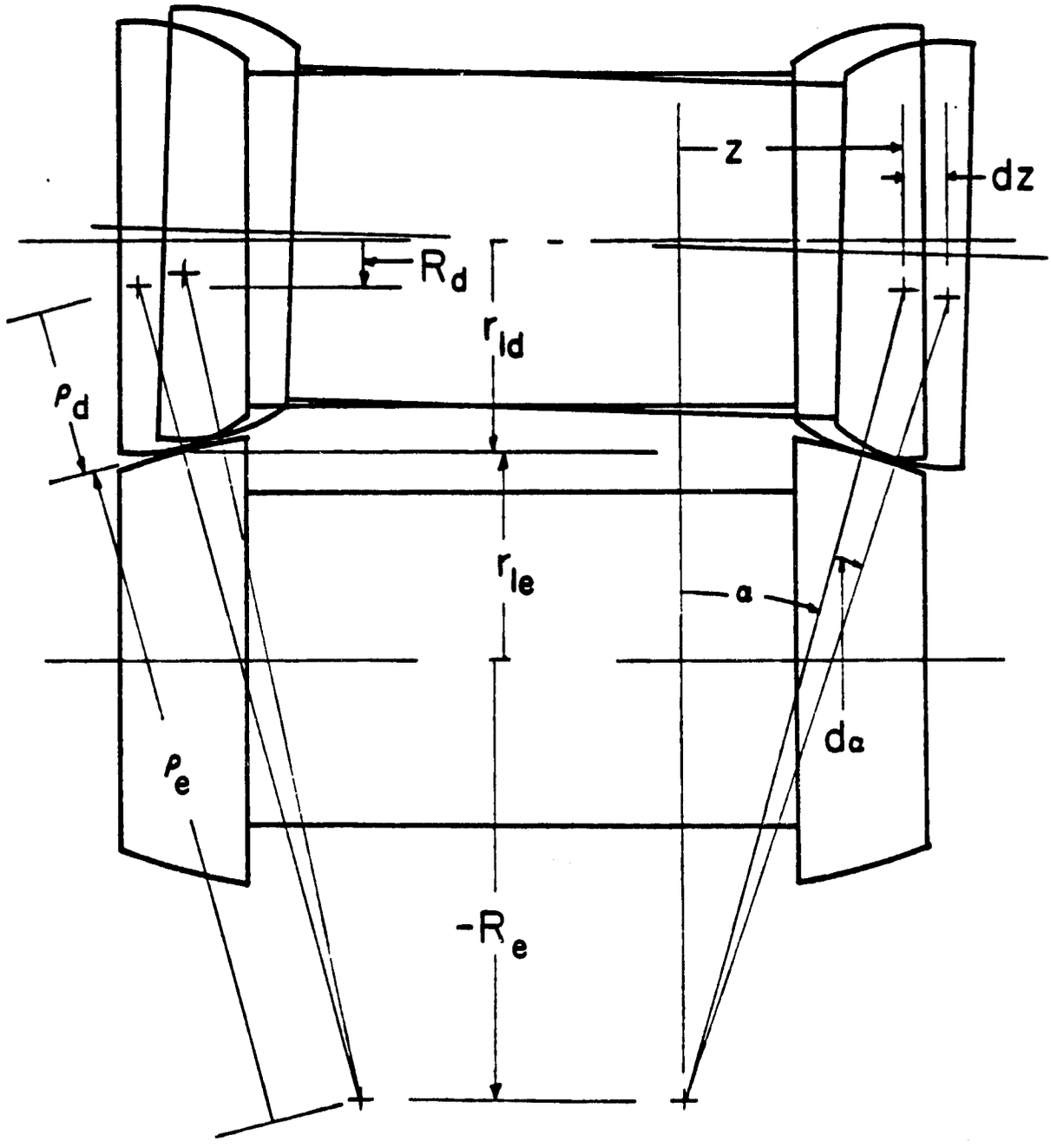

Figure 3 Convex-Convex External Contact Geometry

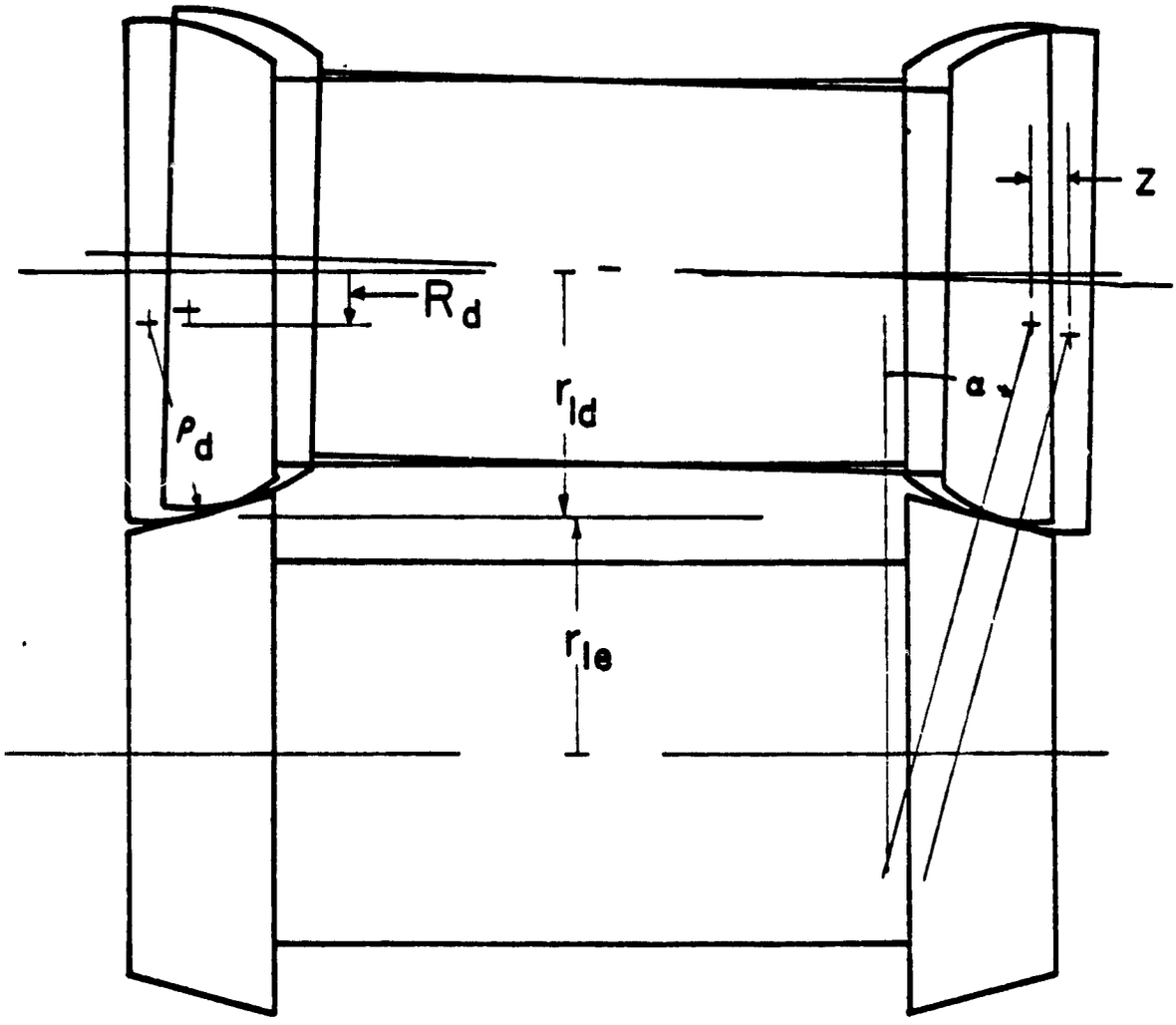

Figure 4 Convex-Straight External Contact Geometry

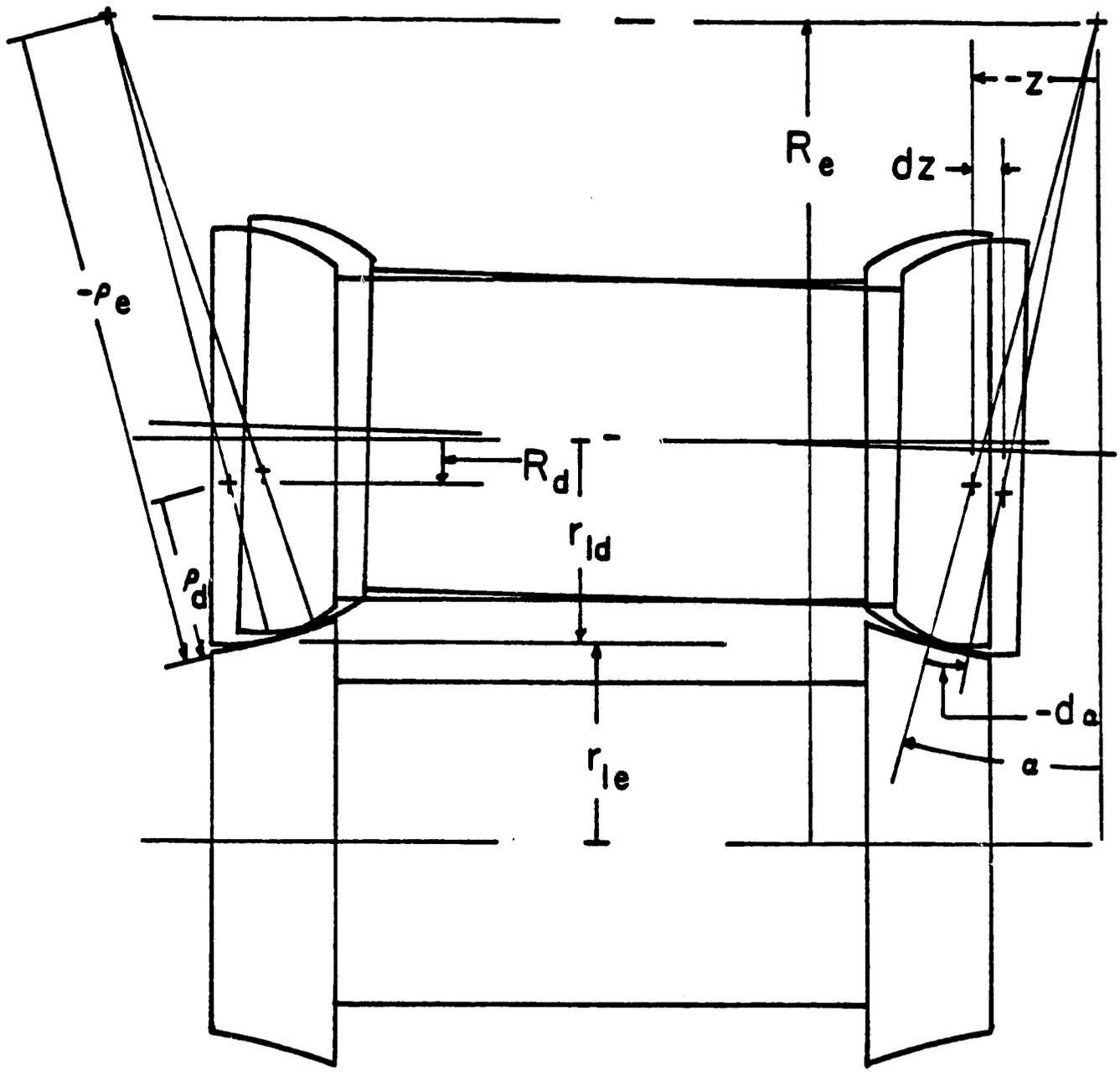

Figure 5 Convex-Concave External Contact Geometry

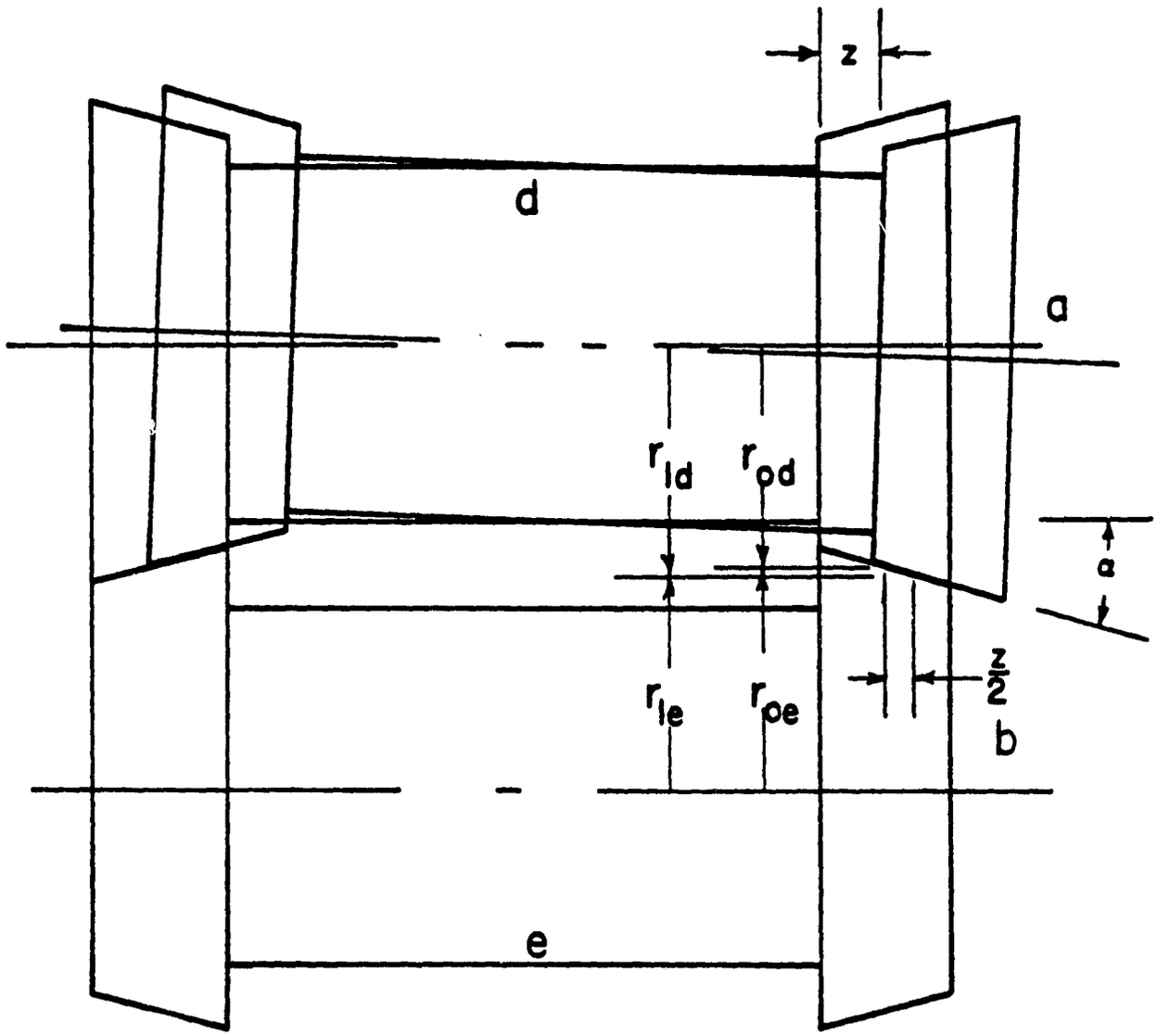

Figure 6 Straight-Straight External Contact Geometry

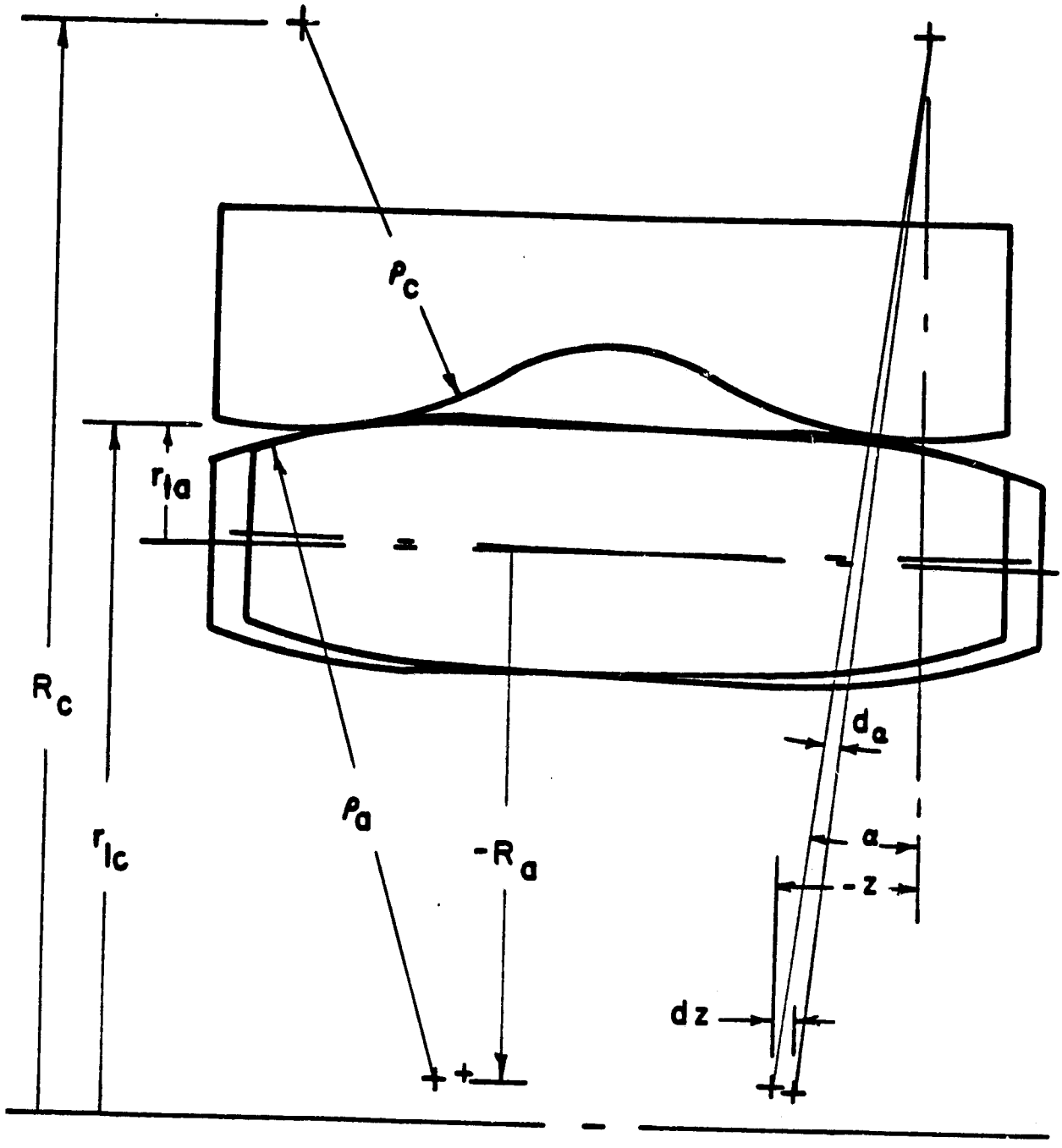

Figure 7 Convex-Convex Outer Race Contact Geometry

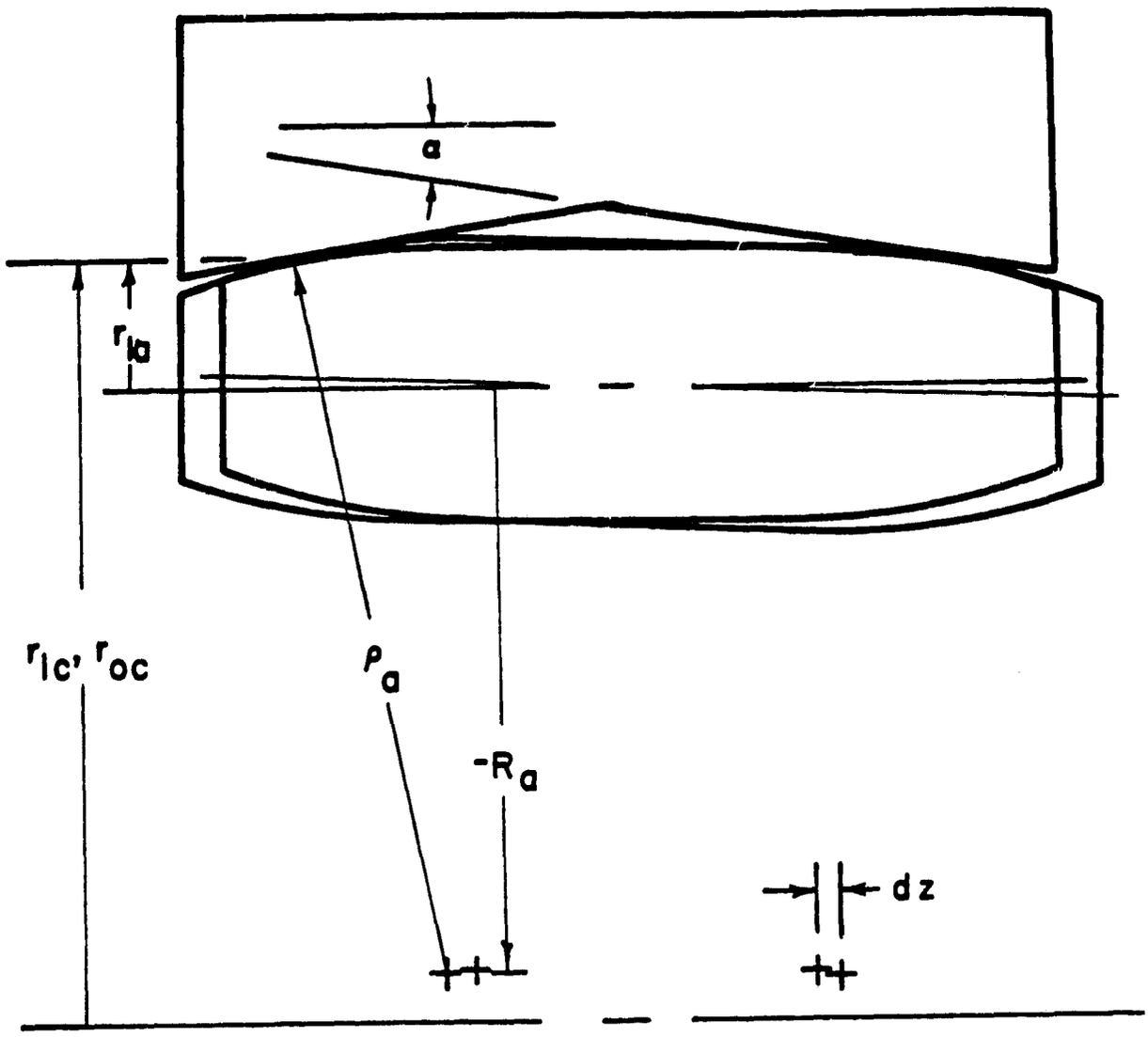

Figure 8 Convex-Straight Outer Race Contact Geometry

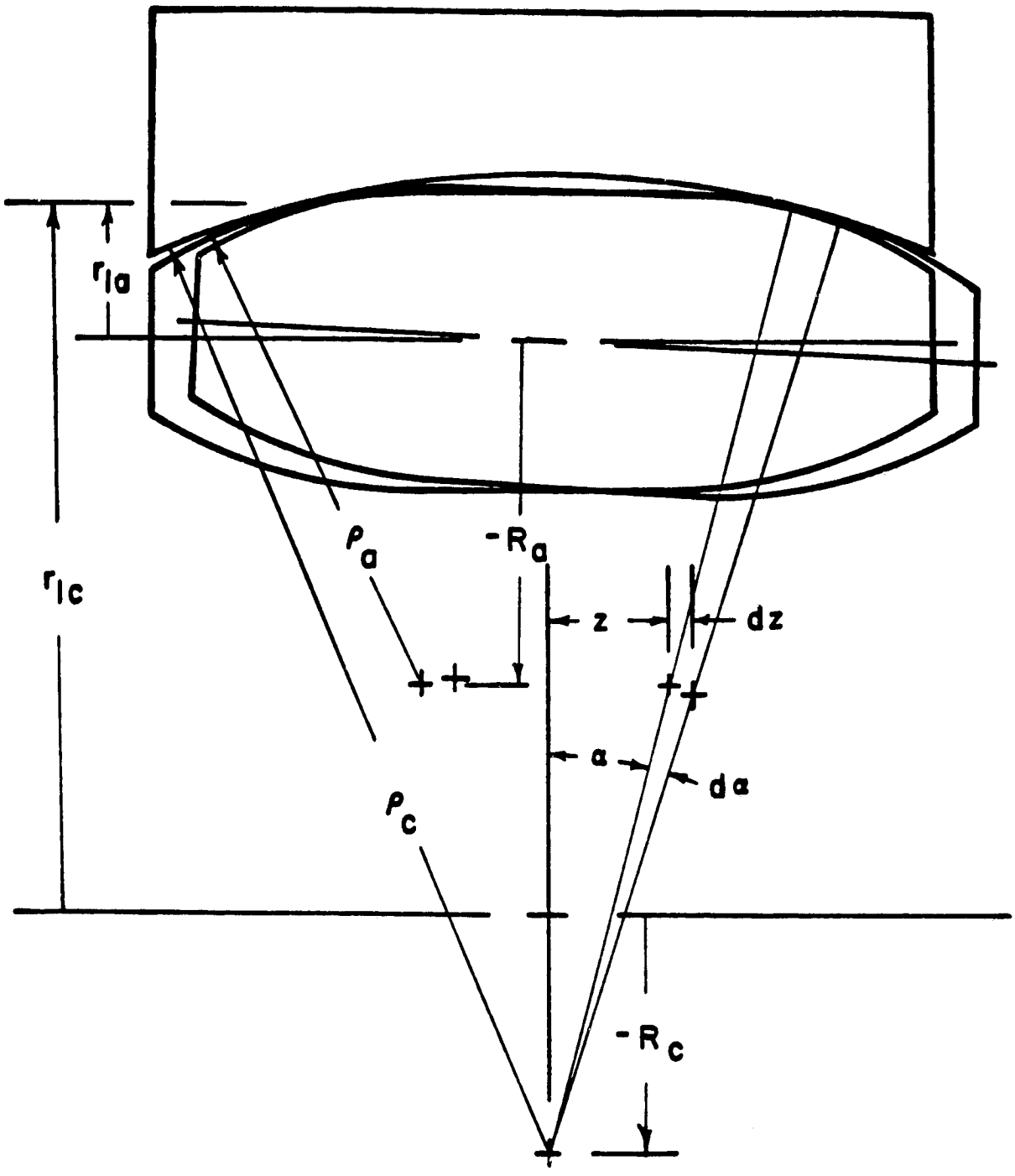

Figure 9 Convex-Concave Outer Race Contact Geometry

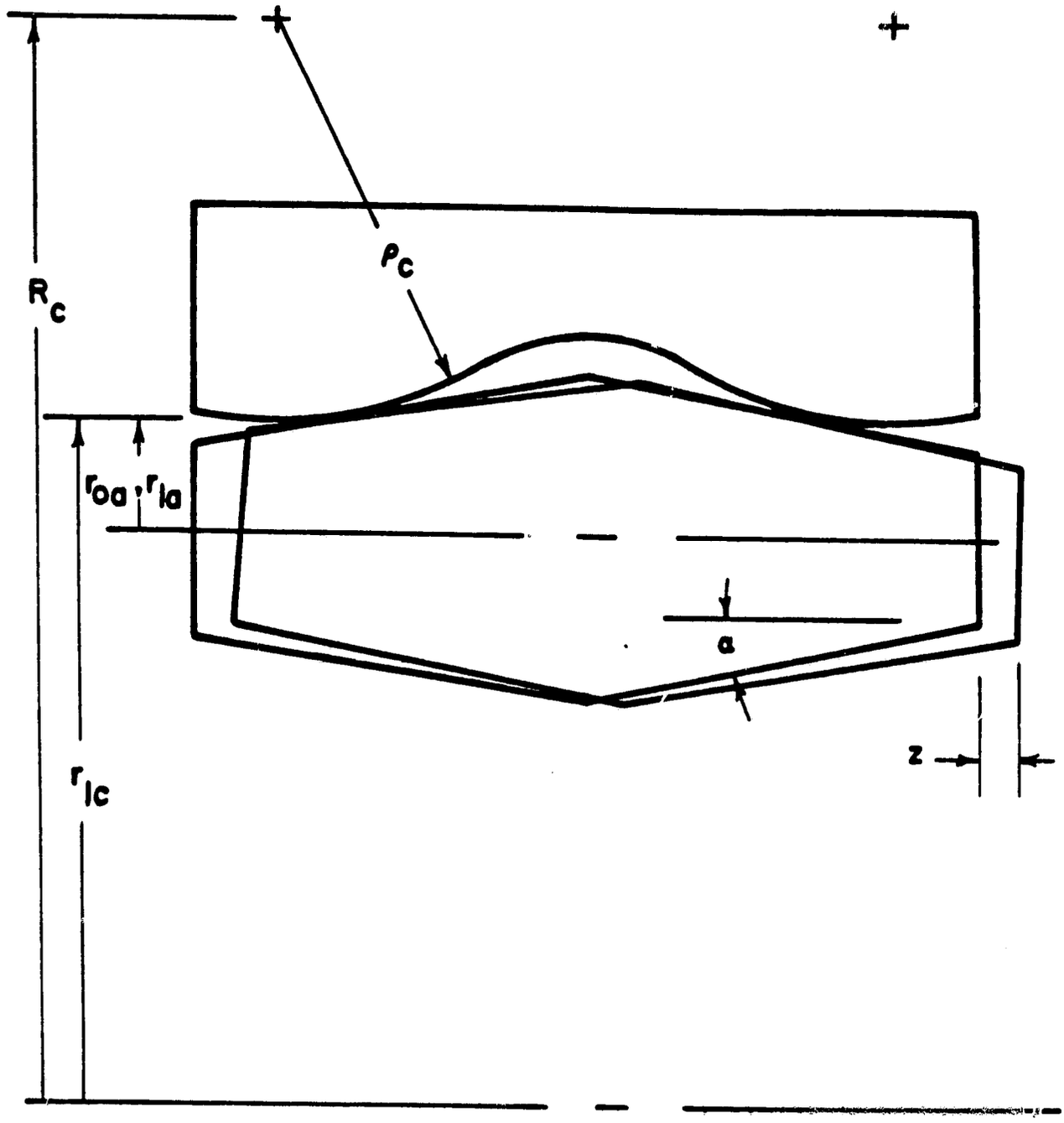

Figure 10 Straight-Convex Outer Race Contact Geometry

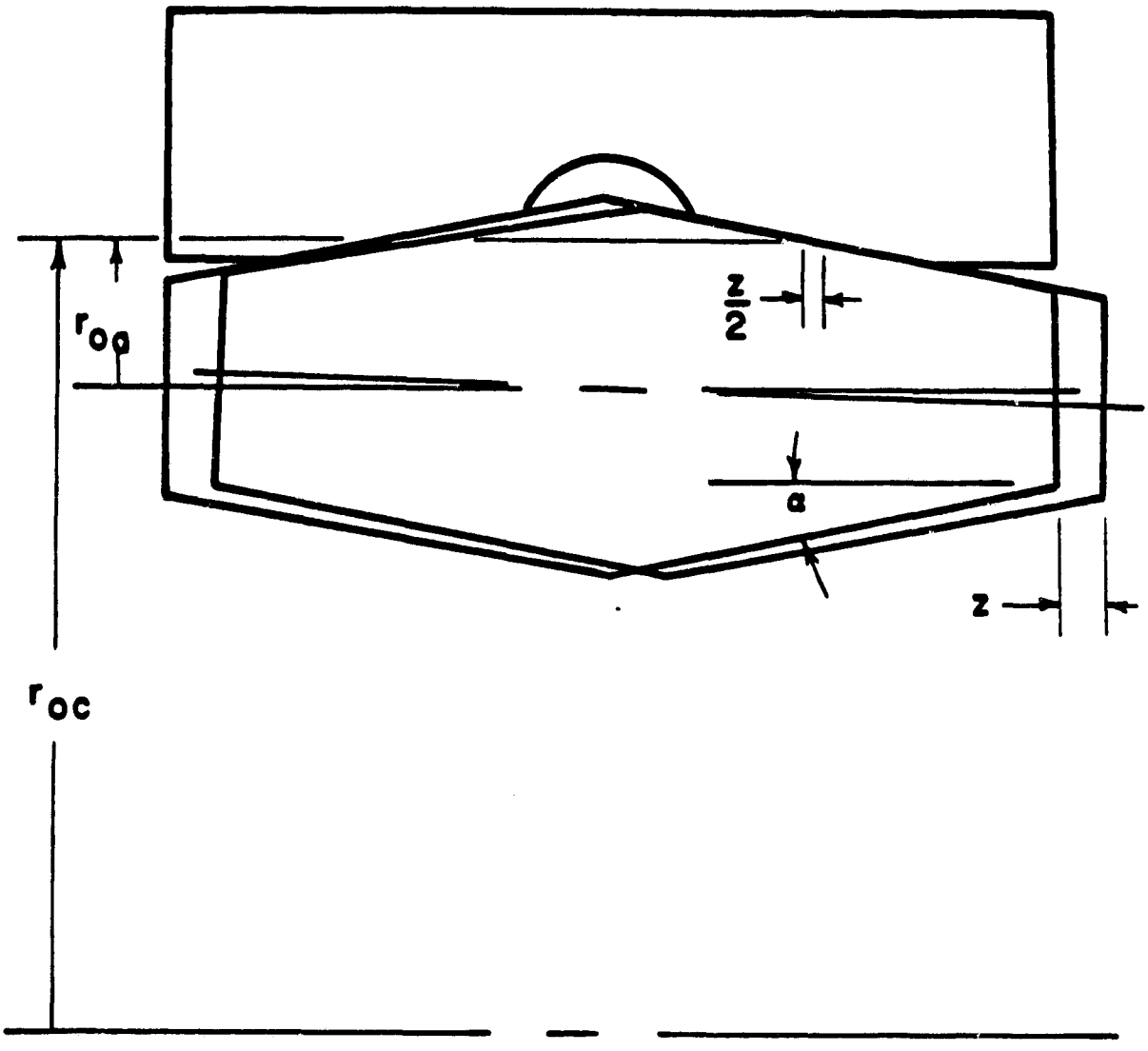

Figure 11 Straight-Straight Outer Race Contact Geometry

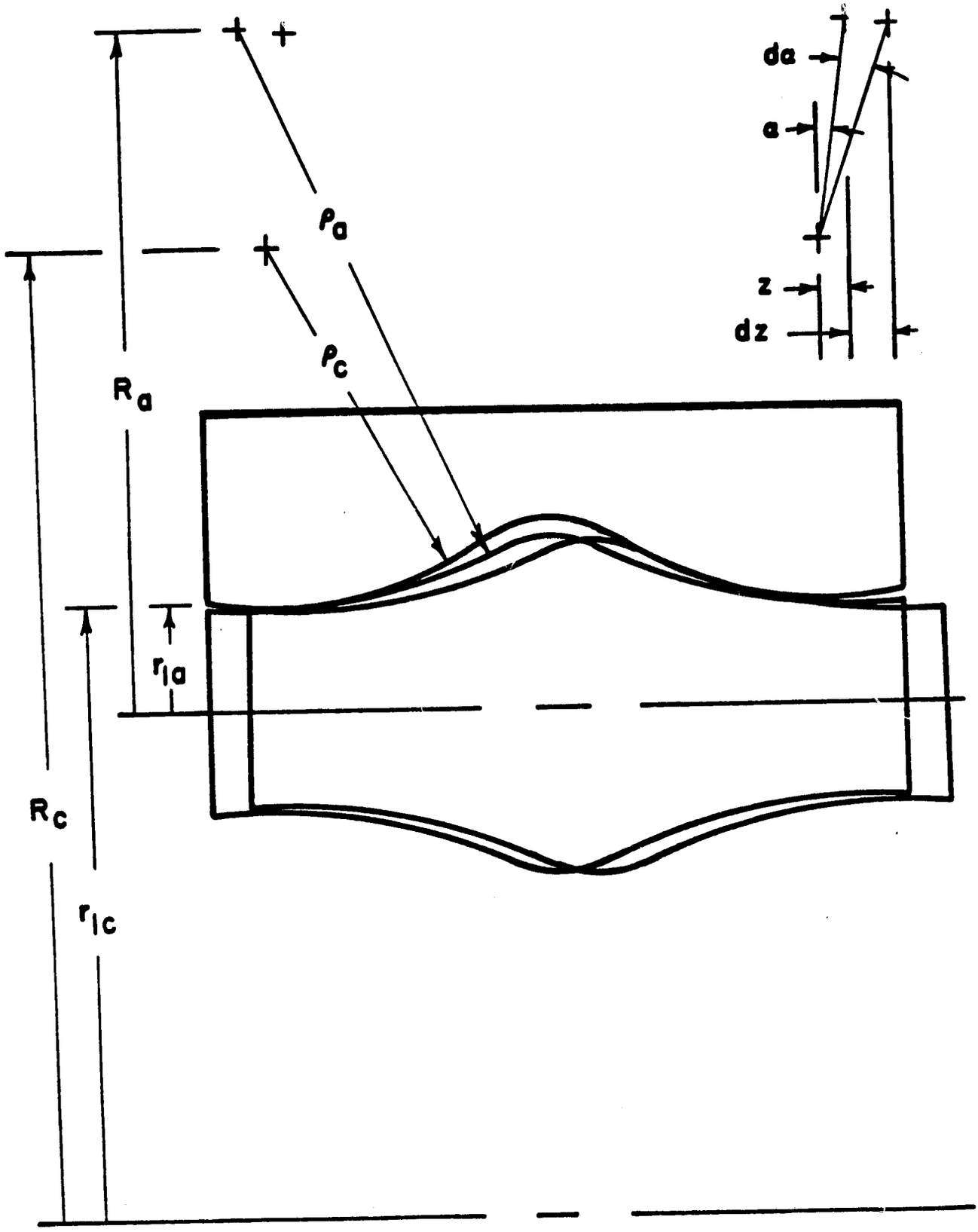

Fiugre 12 Concave-Convex Outer Race Contact Geometry

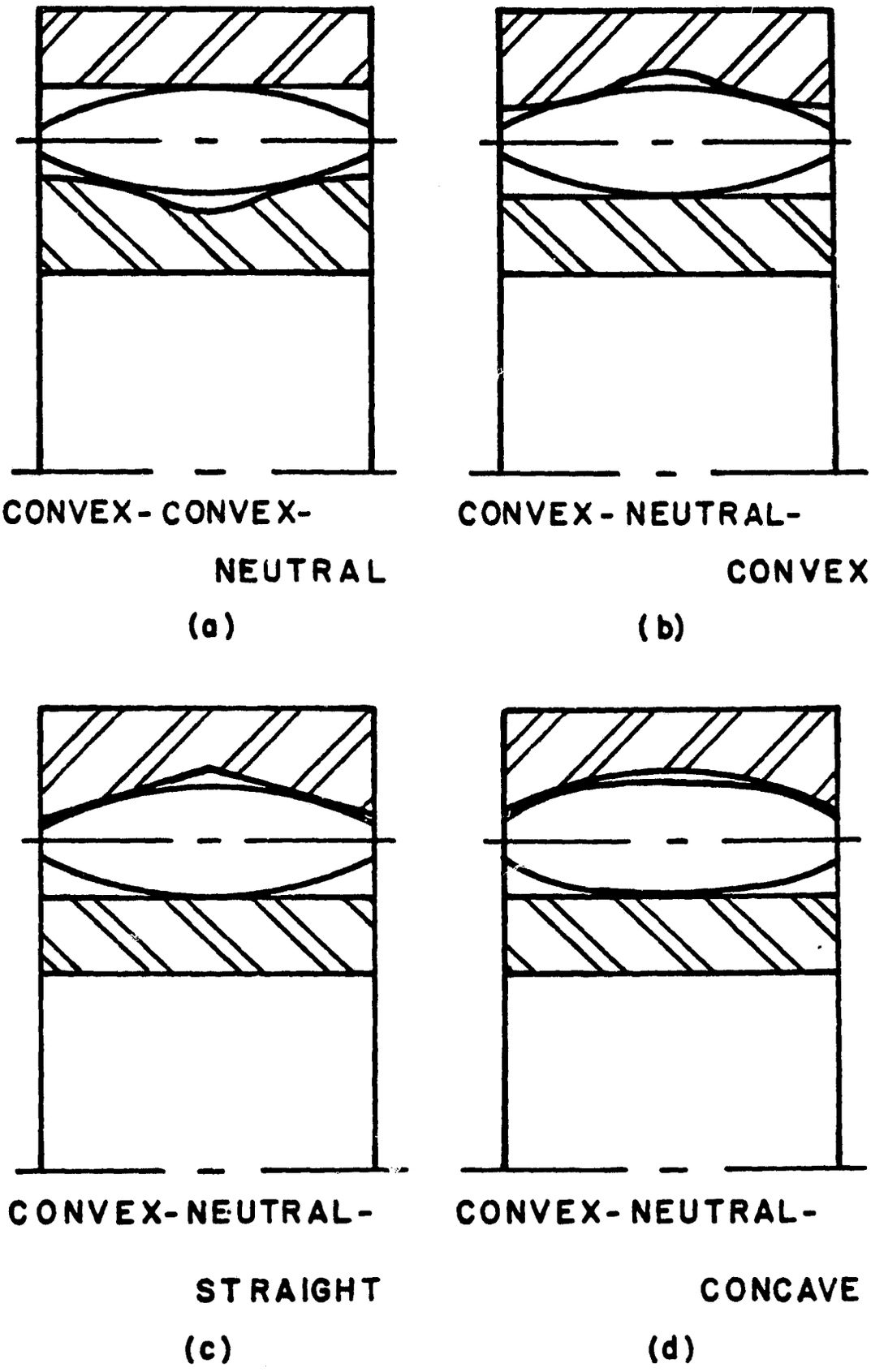

Figure 13 Stable Convex Roller Bearings with Roller, Inner Race and Outer Race Curvatures Noted Respectively

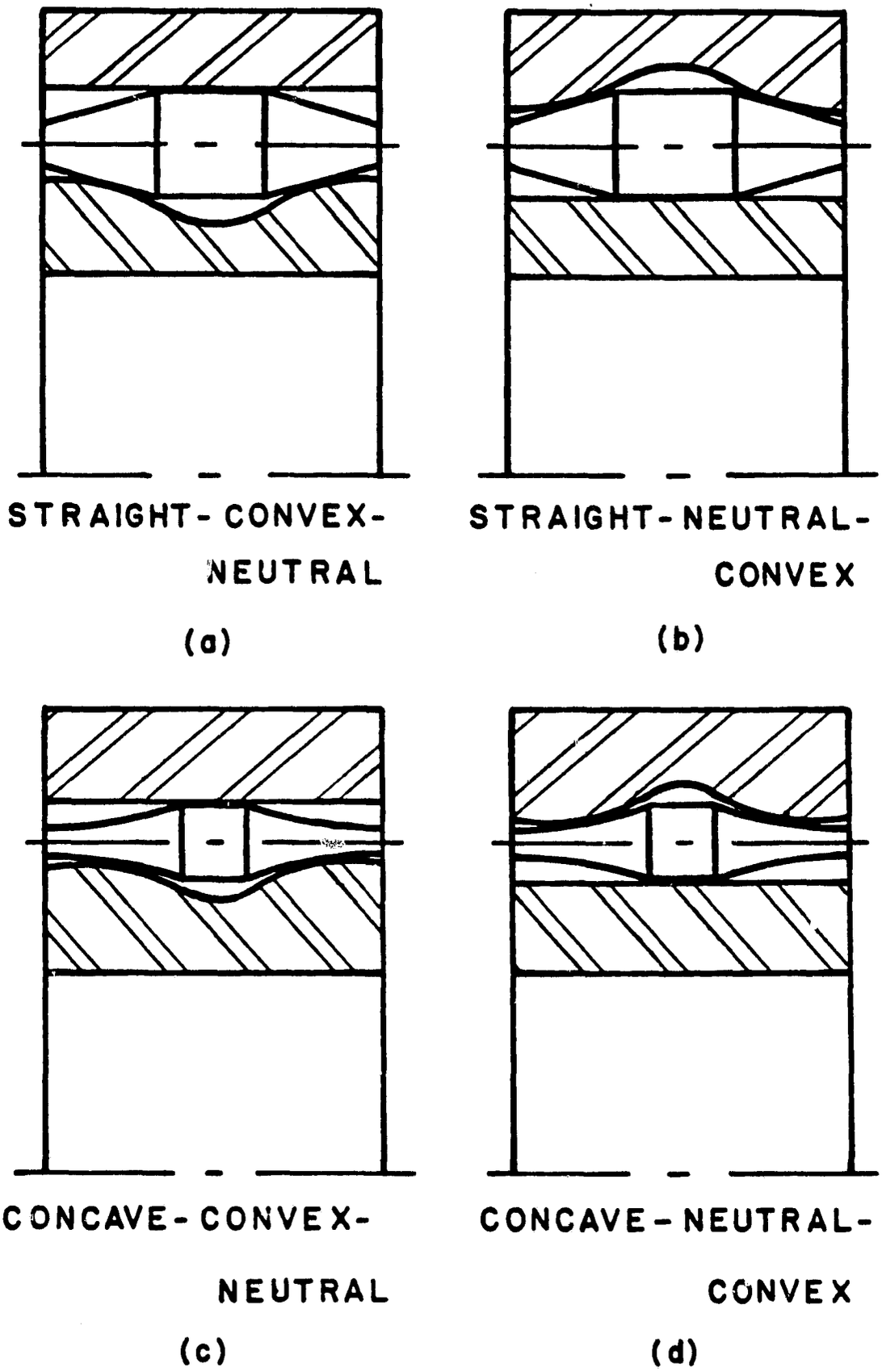

Figure 14 Stable Bearings with Compound Rollers Which are Not Convex With Roller, Inner Race and Outer Race Curvatures Noted Respectively

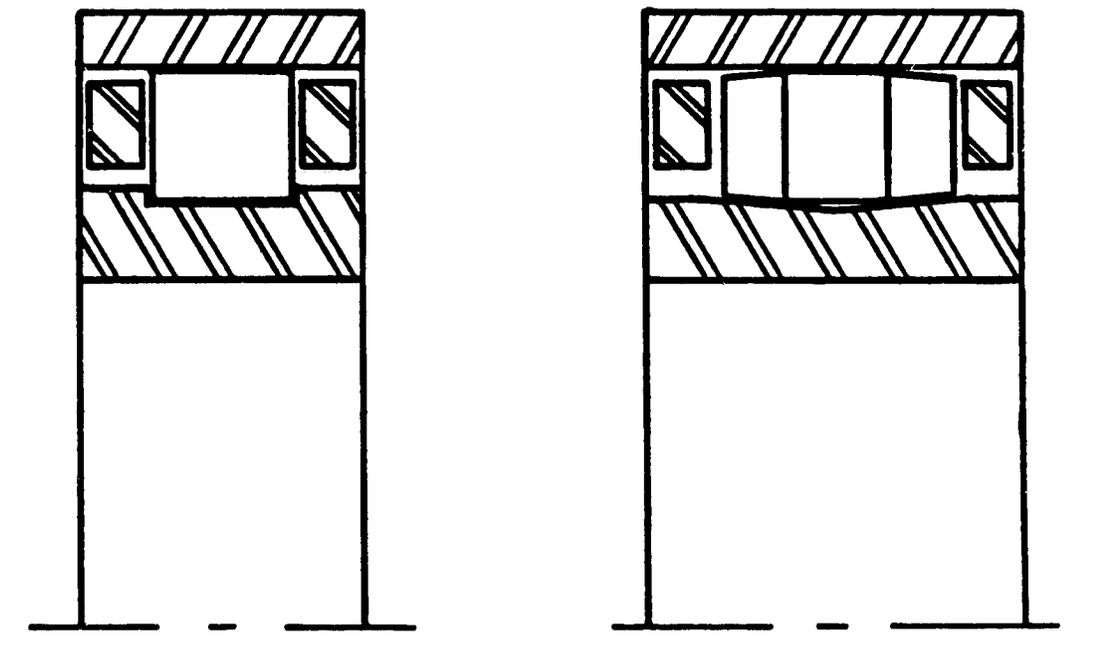

Figure 15 Design Alternative for Roller Bearing